PROGRESS IN PHOTOVOLTAICS: RESEARCH AND APPLICATIONS
Prog. Photovolt: Res. Appl. (2012)
Published online in Wiley Online Library (wileyonlinelibrary.com). DOI: 10.1002/pip.2170

RESEARCH ARTICLE

Method for photovoltaic parameter extraction according to a modified double-diode model

Alexandre José Bühler and Arno Krenzinger*

UFRGS—Universidade Federal do Rio Grande do Sul, Laboratório de Energia Solar, Av. Bento Gonçalves, 9500 Porto Alegre-RS, Brazil

ABSTRACT

The variables presented in the current–voltage equation of a photovoltaic (PV) device are usually called PV parameters. There are several different methods for PV parameter extraction from measured data according to different models. However, many of these methods provide results that do not represent *I–V* curves of thin films devices correctly. This can occur because either the applied model or the PV parameter extraction methods are not suitable. It is also possible that the extracted parameters provide a good mathematical representation of the curves but without physical meaning (e.g. negative series resistance). This work presents a method for PV parameter extraction based on a modified double-diode model. In this model, the ideality factor related to the recombination of the charge carriers in the space-charge region is assumed as a variable. This method has been tested for different *I–V* curves of different PV module technologies providing very good results and parameters with physical meaning in all the cases. Copyright © 2012 John Wiley & Sons, Ltd.

KEYWORDS

photovoltaic module; *I–V* characteristic curve; double-diode model; parameter extraction

***Correspondence**

Arno Krenzinger, UFRGS—Universidade Federal do Rio Grande do Sul, Laboratório de Energia Solar, Av. Bento Gonçalves, 9500 Porto Alegre-RS, Brazil.

E-mail: arno.krenzinger@ufrgs.br

Received 20 December 2010; Revised 27 October 2011; Accepted 23 December 2011

1. INTRODUCTION

The mathematical representation of an *I–V* curve of a photovoltaic device is very important, mainly to be used in simulation software; for instance, to predict the amount of energy, an installation is able to provide under different operational conditions. Besides, the mathematical representation of an *I–V* curve can be very useful to understand physical phenomena that may occur in photovoltaic (PV) devices. This representation can be performed according to different physical models, being the single and double diodes the most used. Both of these models have variables known as PV parameters that must be determined by an appropriated extraction method. Some methods are analytical such as that of Chan and Phang [1], whereas other approaches use numerical methods, such as those of Garrido-Alzar [2] and Sandrolini *et al*. [3]. The use of modified methods is also possible, usually with a larger number of variables. Nishioka *et al*. [4], for example, proposed a three-diode equivalent circuit model taking into account the influence of the grain boundaries and leakage current through the edges for multicrystalline silicon cells.

Although there are several different PV parameter extraction methods, many of these methods are inaccurate in describing *I–V* curves at low irradiance conditions or provide parameters with no physical meaning. Phang *et al*. [5] proposed a versatile and simple analytical method to extract all the five PV parameters from only one measured *I–V* curve according to a single-diode model. Their method provides very good results for both crystalline silicon and thin film devices. However, under some specific conditions, the same method may provide PV parameters with no physical meaning, such as negative series resistance values [6]. In some cases, even at high-irradiance levels, this method may provide significant differences in the series resistance values [7].

Any dark current component of a PN junction is due to recombination of charge carriers somewhere within the device. According to the Shockley theory [8], at high voltages, the recombination predominantly occurs in quasi-neutral regions (surfaces and the bulk regions). The ideality factor related to this component (called in this work 'diffusion current') equals 1. On the other hand, at lower voltages, recombination predominantly occurs in high-field regions (depletion region), and the ideality factor equals 2.

In this work, such component of the dark current is called 'recombination current'. Such values for the ideality diode factor are used in a model known as double-diode model, which usually provides good results when applied in the mathematical representation of crystalline silicon PV curves. However, applied to curves of amorphous devices and other thin film technologies, the double-diode model may not be so good for describing *I–V* curves. One possible reason is that in amorphous silicon, like in other thin films technologies, some physical phenomena take place making the fill factor of the characteristic curve to decrease. One of the possible causes, at least in amorphous materials, consists in the dangling bonds. These defects in the atomic structure correspond to atoms with an incomplete number of electrons in their valence shells because one covalent bond is missing. These incomplete bonds are probable spots for the recombination of free electrons that will not contribute to the photogenerated current.

For a better representation of curves of crystalline and amorphous PV devices, including cells, modules and arrays, the applied model may assume the diode ideality factor related to the recombination as a variable. For this reason, a method was developed for PV parameter extraction based in a modified double-diode model in which the ideality factor for the recombination process may vary. This PV parameter extraction method has been tested in several *I–V* curves of PV devices on the basis of different technologies and in a large range of irradiance and temperature levels, providing very good results as shown in this work.

2. DESCRIPTION OF THE METHOD

The equivalent electrical circuit for a PV cell according to the modified double-diode model is shown in Figure 1 where I is the solar cell current, V is the solar cell voltage, I_{PH} is the photocurrent, I_D is the diffusion current of the charge carriers, I_R is the recombination current of the charge carriers, I_{SH} is leakage current, r_{SH} is the cell shunt resistance and r_S is the cell series resistance.

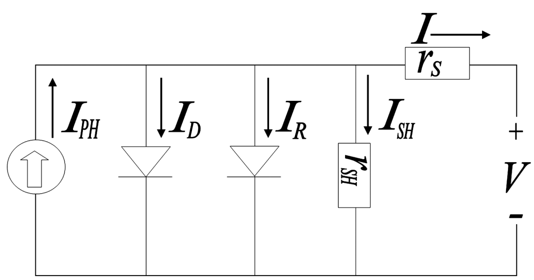

Figure 1. Equivalent electrical circuit of a solar cell according to the double-diode model.

According to the equivalent circuit shown in Figure 1, the current supplied by a solar cell in a specific condition of temperature and irradiance can be described by Equation (1).

$$I = I_{PH} - I_{D0}\left\{\exp\left[\frac{e(V + Ir_S)}{k_B T}\right] - 1\right\} - I_{R0}\left\{\exp\left[\frac{e(V + Ir_S)}{m_R k_B T}\right] - 1\right\} - \frac{V + Ir_S}{r_{SH}} \tag{1}$$

where e is the electron charge, k_B is the Boltzmann constant, m_R is the ideality factor for the recombination process, T is the temperature of the cell, and I_{D0} and I_{R0} are the pre-exponential factors for the diffusion and recombination current of the charge carriers

Equation (1) is valid for a solar cell. In the case of PV modules, considering the modules as associations of identical cells and taking into account some considerations, a similar equation can be assumed.

By defining V_T in Equation (2), where N_J represents the number of cells in series multiplied by the number of PN junctions (in each cell) and substituting V_T in Equation (1), Equation (3) that describes the current–voltage relationship in a PV module is obtained.

$$V_T = \frac{N_J k_B T}{e} \tag{2}$$

$$I = I_{PH} - I_{D0}\left\{\exp\left[\frac{V + IR_S}{V_T}\right] - 1\right\} - I_{R0}\left\{\exp\left[\frac{V + IR_S}{m_R V_T}\right] - 1\right\} - \frac{V + IR_S}{R_{SH}} \tag{3}$$

where R_S and R_{SH} correspond to the series and shunt resistance of a PV module.

Applying the short-circuit condition ($I = I_{SC}$ and $V = 0$) in Equation (3), a good approximation for I_{PH} is obtained:

$$I_{PH} = I_{SC}\left(1 + \frac{R_S}{R_{SH}}\right) + I_{D0}\left[\exp\left(\frac{I_{SC}R_S}{V_T}\right) - 1\right] + I_{R0}\left[\exp\left(\frac{I_{SC}R_S}{m_R V_T}\right) - 1\right] \cong I_{SC}\left(1 + \frac{R_S}{R_{SH}}\right) \tag{4}$$

where I_{SC} is the short-circuit current.

Applying the condition at the maximum power point, where the voltage is V_M and the current is I_M, and replacing I_{PH} from Equation (4), one obtains the following:

$$I_{R0} = \frac{\left[(I_{SC} - I_M)\left(1 + \frac{R_S}{R_{SH}}\right) - \frac{V_M}{R_{SH}}\right] - I_{D0}\left[\exp\left(\frac{V_M + I_M R_S}{V_T}\right) - \exp\left(\frac{I_{SC}R_S}{V_T}\right)\right]}{\left[\exp\left(\frac{V_M + I_M R_S}{m_R V_T}\right) - \exp\left(\frac{I_{SC}R_S}{m_R V_T}\right)\right]} \tag{5}$$

DOI: 10.1002/pip

Applying the open-circuit condition ($I = 0$ and $V = V_{OC}$) in Equation (3) and also replacing I_{PH} from Equation (4), one obtains the following:

$$I_{D0} = \frac{\left[I_{SC}\left(1+\frac{R_S}{R_{SH}}\right) - \frac{V_{OC}}{R_{SH}}\right] - I_{R0}\left[\exp\left(\frac{V_{OC}}{m_R V_T}\right) - \exp\left(\frac{I_{SC}R_S}{m_R V_T}\right)\right]}{\left[\exp\left(\frac{V_{OC}}{V_T}\right) - \exp\left(\frac{I_{SC}R_S}{V_T}\right)\right]} \tag{6}$$

$$R_S = -\left.\frac{\partial V}{\partial I}\right|_{OC} - \frac{V_T}{I_{D0}\exp\left(\frac{V_{OC}}{V_T}\right) + \frac{I_{R0}}{m_R}\exp\left(\frac{V_{OC}}{m_R V_T}\right) + \frac{V_T}{R_{SH}}} \tag{11}$$

The shunt resistance is considered approximately equal to the negative value of the derivative of V as a function of I at the short-circuit point ($-\partial V/\partial I|_{V=0} = R_{SH}$) such as shown in Equation (12).

$$\frac{1}{R_{SH}} = -\left\{\frac{1}{\left.\frac{\partial V}{\partial I}\right|_{SC}} + R_S + \frac{1}{V_T}\left[I_{D0}\exp\left(\frac{I_{SC}R_S}{V_T}\right) + \frac{I_{R0}}{m_R}\exp\left(\frac{I_{SC}R_S}{m_R V_T}\right)\right]\right\} \cong \frac{1}{-\left.\frac{\partial V}{\partial I}\right|_{SC}} \tag{12}$$

Equations (5) and (6) constitute a system of equations so that I_{R0} and I_{D0} can be obtained. To simplify the determination of the pre-exponential factor Equations (5) and (6) are redefined, respectively, as follows:

$$I_{R0} = I_{R1} - f_{D0}I_{D0} \tag{7}$$

$$I_{D0} = I_{D1} - f_{R0}I_{R0} \tag{8}$$

where

$$I_{R1} = \frac{\left[(I_{SC}-I_M)\left(1+\frac{R_S}{R_{SH}}\right) - \frac{V_M}{R_{SH}}\right]}{\left[\exp\left(\frac{V_M+I_M R_S}{m_R V_T}\right) - \exp\left(\frac{I_{SC}R_S}{m_R V_T}\right)\right]} \text{ and } f_{D0} = \frac{\left[\exp\left(\frac{V_M+I_M R_S}{V_T}\right) - \exp\left(\frac{I_{SC}R_S}{V_T}\right)\right]}{\left[\exp\left(\frac{V_M+I_M R_S}{m_R V_T}\right) - \exp\left(\frac{I_{SC}R_S}{m_R V_T}\right)\right]}$$

$$I_{D1} = \frac{\left[I_{SC}\left(1+\frac{R_S}{R_{SH}}\right) - \frac{V_{OC}}{R_{SH}}\right]}{\left[\exp\left(\frac{V_{OC}}{V_T}\right) - \exp\left(\frac{I_{SC}R_S}{V_T}\right)\right]} \text{ and } f_{R0} = \frac{\left[\exp\left(\frac{V_{OC}}{m_R V_T}\right) - \exp\left(\frac{I_{SC}R_S}{m_R V_T}\right)\right]}{\left[\exp\left(\frac{V_{OC}}{V_T}\right) - \exp\left(\frac{I_{SC}R_S}{V_T}\right)\right]}$$

From Equations (7) and (8), one obtains I_{R0} and consequently I_{D0}.

$$I_{R0} = \frac{I_{R1} - f_{D0}I_{D1}}{1 - f_{D0}f_{R0}} \tag{9}$$

Equation (9) will provide I_{R0} once R_S is known and m_R has a pre-established value. Once I_{R0} is calculated, its value is used to calculate I_{D0} through Equation (8). To determine R_S and m_R by an iterative method, another equation is necessary, whose origin is shown as follows:

Differentiating Equation (3) with respect to I and isolating $\partial V/\partial I$,

$$-\frac{\partial V}{\partial I} = R_S + \frac{V_T}{I_{D0}\exp\left(\frac{V+IR_S}{V_T}\right) + \frac{I_{R0}}{m_R}\exp\left(\frac{V+IR_S}{m_R V_T}\right) + \frac{V_T}{R_{SH}}} \tag{10}$$

Applying the open-circuit condition in Equation (10) and isolating R_S,

It is known that R_S affects the slope of the I–V curve nearby the open-circuit region. However, part of the slope of the I–V curve is due to its exponential behaviour, and then R_S must be smaller than the module's derivative of V as function of I at $V = V_{OC}$. Therefore, this derivative is the initial guess for the R_S calculation procedure. It is also assumed that the R_S calculation procedure only converges when a suitable value of m_R is chosen. However, a range of m_R values is possible, and then a comparison between the calculated and measured curves is necessary to find the best value for m_R. Thus, the procedure for the determination of all PV parameters according to the modified double-diode model is the following:

(i) The 'electrical PV parameters', such as V_{OC} and I_{SC}, are extracted from the measured I–V curve. The post-processing procedure applied to this extraction is presented after the PV parameters determination procedure.
(ii) An initial value for $m_R = 2$ is set.
(iii) An initial error ($Er_0 = 10$) is set. The set value must be large enough to guarantee that the first calculated error be smaller than the set one. This error corresponds to a relative difference between the R_S guess and the R_S calculated (Equation 11).
(iv) An initial guess for $R_S = -\partial V/\partial I|_{V=V_{oc}}$ is set.
(v) The photocurrent is calculated using Equation (4).
(vi) Using Equation (9), I_{R0} is calculated.
(vii) Using Equation (8), I_{D0} is calculated
(viii) With I_{R0} and I_{D0} already calculated and with the initial guess for m_R set, R_S is calculated by using Equation (11).
(ix) The error between the R_S guess and the R_S calculated is evaluated.
(x) If the calculated error in this step is larger than the error in the previous step, then a new value of m_R (the previous value plus an increment) is set and the procedure goes to step (iii). In this work, an increment of 0.01 for m_R was set.
(xi) If the calculated error in this step is smaller than the error in the previous step, then its value is compared with a minimum value for convergence. In this work, the value for convergence was set to 0,001.

(xii) If the error is larger than the convergence value, then the calculated R_S is taken as the new R_S guess and the procedure goes to step (v).

(xiii) With the use of the PV parameters obtained until this step, two values of current are calculated according to the proposed method. The calculated values of current are related to measured values of voltage equal to $(2V_M - V_{OC})$ and $0.5(V_M + V_{OC})$.

(xiv) The root mean square deviation (RMSD) between the calculated and measured currents is determined.

(xv) A previous value for m_R plus an increment is established, and steps (iii)–(xiv) are performed again giving a new value of RMSD. The previous RMSD is compared with the actual RMSD. If the RMSD become smaller, then all the steps from (iii) to (xiv) are performed again and so on while the RMSD decreases. When the RMSD increases, the method finishes and all the PV parameters that provide the best fit for the I–V curve are taken from the previous step. The increment of m_R is the same as that in step (x).

To extract the PV parameters according to the proposed method, some initial data are needed such as V_{OC} and I_{SC}. The better the determination of these data, the better is the final result in the PV parameter extraction. Thus, a post-processing procedure has to be applied in the raw measured data. The post-processing applied to perform this work consists basically of the following:

V_{OC} region From the measured data, I–V pairs with current between 0 and $0.2\,I_{SCM}$ are selected, and a linear least-square regression is applied providing the value of V_{OC} and the slope of the curve in this region. I_{SCM} corresponds to the measured current at the voltage nearest to 0 V.

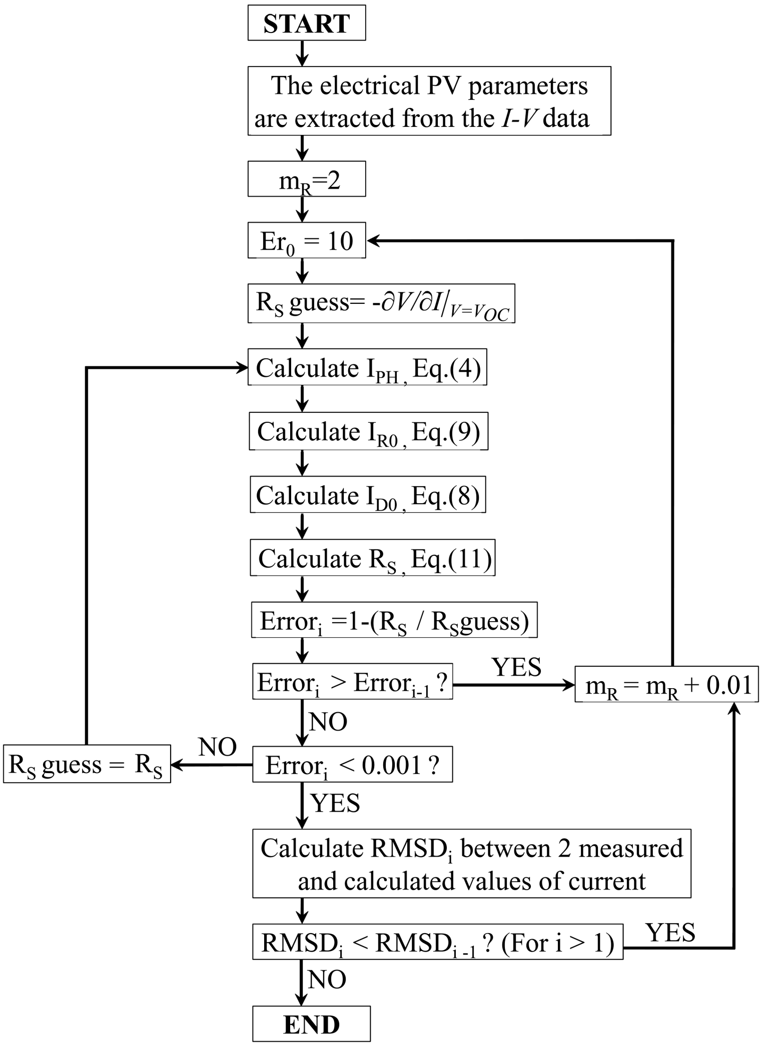

Figure 2. Flowchart of the procedure for photovoltaic (PV) parameter extraction according to a modified double-diode model. RMSD, root mean square deviation.

I_{SC} region From the measured data, *I–V* pairs with voltage between 0 and 0.2 V_{OCM} are selected, and a linear least-square regression is applied providing the value of I_{SC} and the slope of the curve in this region. V_{OCM} corresponds to the measured voltage at the current nearest to 0 A.

P_M region From the measured data, *I–V* pairs with voltage between V_{MD} and V_{MU} are selected, and a fourth-order polynomial least-square regression is applied providing the values of V_M and I_M. The term V_{MD} is equal to $2V_{MM} - V_{OC}$, and the term V_{MU} is equal to $0.5(V_{MM} + V_{OC})$ where V_{MM} corresponds to the voltage of the maximum measured power point. This interval used to calculate V_M and I_M guarantees that regardless the value of fill factor of the *I–V* curve, the fitting of a fourth-order polynomial least-square regression will provide a very accurate result.

Figure 2 shows a flowchart regarding the proposed extraction PV parameters according to a modified double-diode model. Figure 3 shows two examples of the iterative process for R_S determination. The examples shown in Figure 3 are related to *I–V* curves of an amorphous silicon single junction (a-Si) module and a Copper–Indium–Diselenide (CIS) module. It is possible to see that in both cases shown in Figure 3, the iterative process for R_S determination reaches the convergence value in a low number of iterations.

Figure 4 shows the relationship between values of m_R and the RMSD for two different measured and calculated currents (related to V_{MD} and V_{MU}). The *I–V* curves used to generate the examples in Figure 4 are the same used in

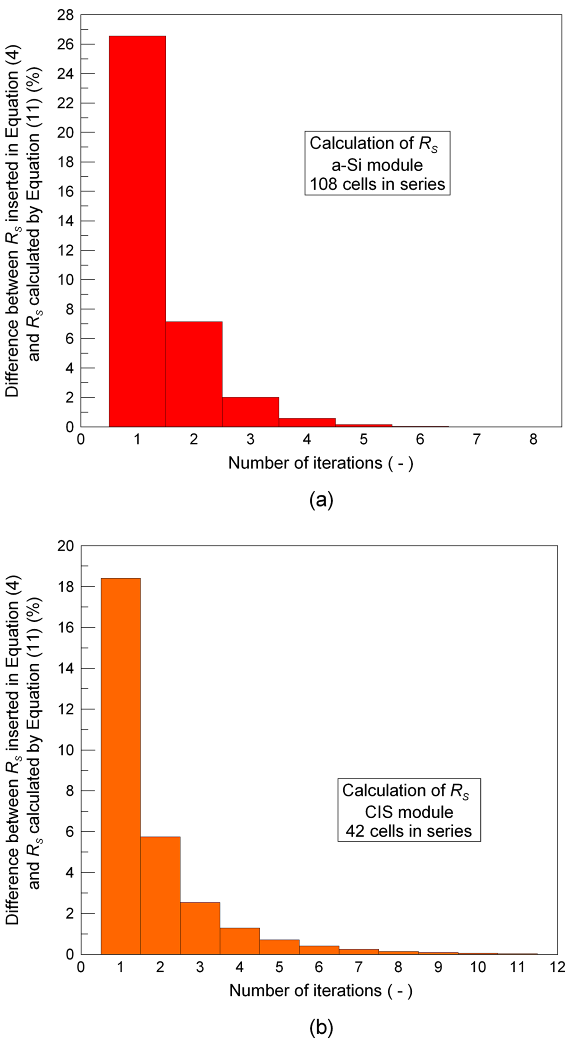

Figure 3. Examples of the iterative method for R_S determination for an *I–V* curve of a module: (a) amorphous silicon single junction (a-Si) and (b) Copper–Indium–Diselenide (CIS).

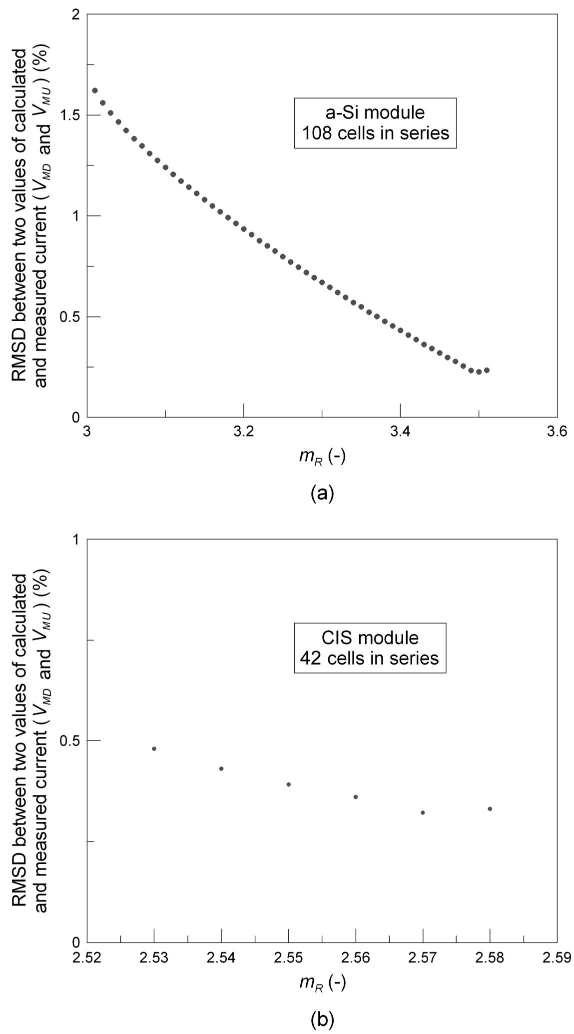

Figure 4. >Relationship between values of m_R and the root mean square deviation (RMSD) for two measured and calculated values of current, related to V_{MD} and V_{MU} for *I–V* curves of (a) amorphous silicon single junction (a-Si) module and (b) Copper–Indium–Diselenide (CIS) module.

Figure 3. In Figure 4, only the m_R values that provide convergence to the R_S calculation are shown.

3. APPLICATION OF THE METHOD

To test the proposed method to PV parameter extraction according to the modified double-diode model, *I–V* curves of PV modules of different technologies were measured in several temperature and irradiance conditions.

Part of the analysed *I–V* curves was measured in the facilities of the CIEMAT (Centro de Investigaciones Energéticas, Medioambientales y Tecnológicas), Public Research Agency of the Ministry of Science and Innovation of Spain. These curves were measured under natural illumination with digital voltmeters (4.5 digits resolution for current and voltage measurements). The temperature measurement of the modules was performed by means of a thermocouple attached on the back surface of the modules. The temperature of the modules was measured with a 0.1 °C resolution. The other part of the curves used in this work was measured in the facilities of the Labsol, Solar Energy Laboratory of the Universidade Federal do Rio Grande do Sul, Brazil. Such curves were also measured under natural illumination with digital voltmeters (6.5 digits resolution for current and voltage). The temperature measurement was also performed on the back surface of the modules but using a Pt100 sensor. The total time for the acquisition of 500 points was around 100 ms.

Modules of the following technologies were measured: CIS, a-Si, Sanyo HIT (heterojunction with intrinsic thin layer), cadmium telluride (CdTe), multicrystalline silicon, monocrystalline silicon, amorphous silicon double junction and amorphous silicon triple junction. Figures 5–12 show the measured and calculated curves with the extracted PV parameters according to the proposed method.

Taking into account that the modified double-diode current–voltage equation corresponds to a transcendental equation, the bisection method was applied to make possible to calculate values of current related to the same measured values of voltage.

Tables I–VIII present the PV parameters obtained by the application of the proposed method, the conditions in which the *I–V* curves were measured and the RMSD for all the *I-V* curve that is obtained by the comparison of each measured and calculated current. The RMSD for each *I–V* curve is shown in terms of percentage of I_{SC} (the value of I_{SC} of the same curve).

It is possible to see in Figures 5–12 that the proposed method provided a very good fit in all the *I–V* curves analysed in this work. The accuracy of the fitting precision does not depend on the cell technology and the irradiation and temperature condition in which the curve was measured. In the case of the CdTe module, the fitting of the curves had an RMSD slightly larger than 1% of I_{SC}. In all other cases, the RMSD was smaller than 1% of I_{SC}, which represents the good quality of the PV extracted parameters. RMSD values are also due to experimental data

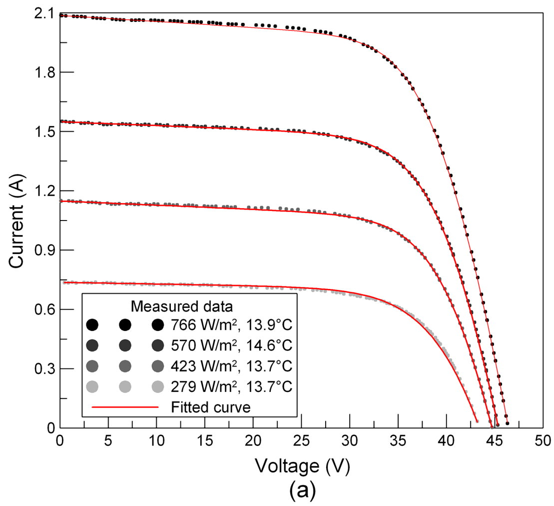

Figure 5. Measured curves in different irradiation and temperature conditions and calculated curves according the proposed method for a Copper–Indium–Diselenide module.

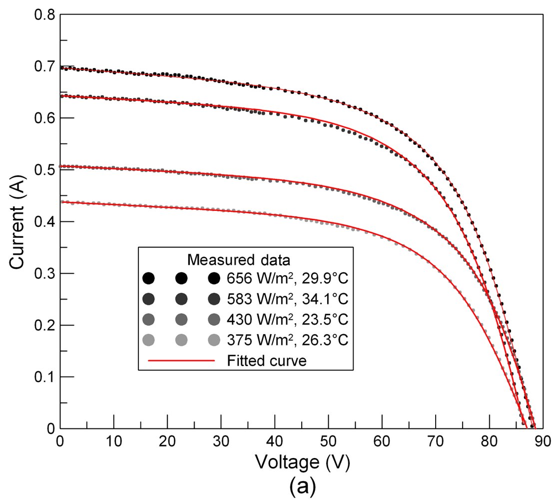

Figure 6. Measured data in different irradiation and temperature conditions and calculated curves according the proposed method for an amorphous silicon single junction module.

noise. To estimate the effect of the noise to the signal of the measurements, the curves were compared with their moving average function. Therefore, the RMSD shown in the Tables I–VIII do not show the influence of the data noise in the fitting of the *I–V* curves. It was found that in average, the role of data noise in the *I–V* curves analysed in this work is about only 0.1% of the total RMSD. In fact, the most important part of the *I–V* curve that increases the RMSD values is the region between the maximum power and the open-circuit voltage. This occurs because even a very small difference between the measured and calculated voltages gives an appreciable difference in current.

By analysing the PV parameters shown in Tables I–VIII, it is possible to see that according to the applied method, the

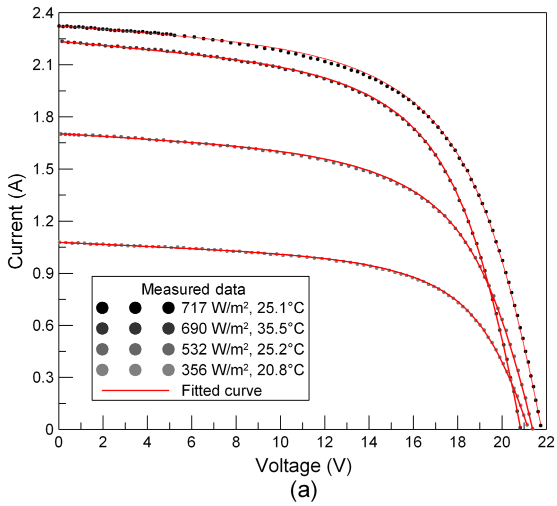

Figure 7. Measured data in different irradiation and temperature conditions and calculated curves according the proposed method for an amorphous silicon double junction module.

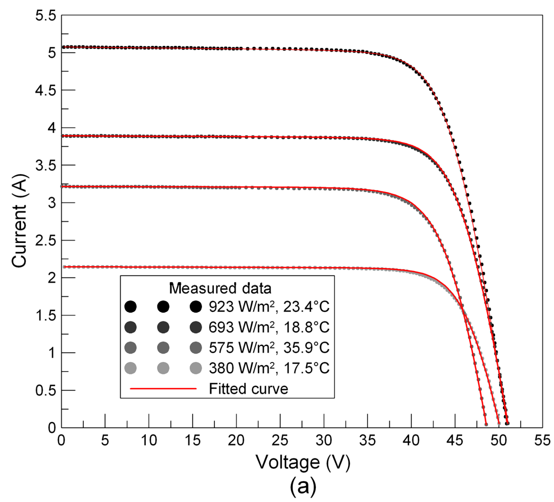

Figure 8. Measured data in different irradiation and temperature conditions and calculated curves according the proposed method for a heterojunction with intrinsic thin layer module.

m_R factor has values equal to 2 for crystalline silicon technology (which includes the HIT technology) and values larger than 2 for thin film technology.

All the mathematical process involved in the proposed method for PV parameter extraction can be considered as a hybrid analytical-numerical method. The main highlights are as follows:

- The method uses always the same initial values for m_R and R_S.
- The determined value of R_S can be considered as a physical internal resistance in the PV device and not only a mathematic parameter of fitting.

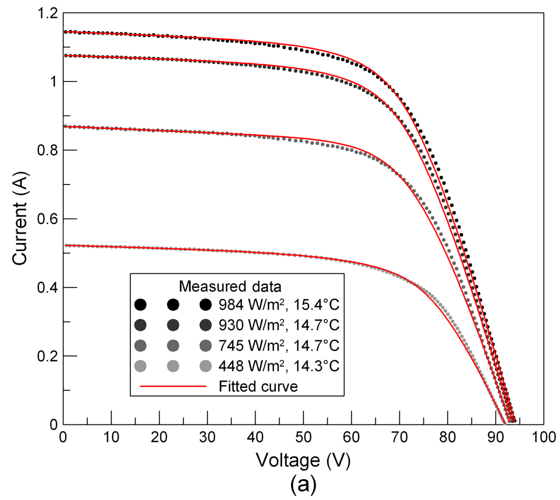

Figure 9. Measured data in different irradiation and temperature conditions and calculated curves according the proposed method for a CdS/CdTe module.

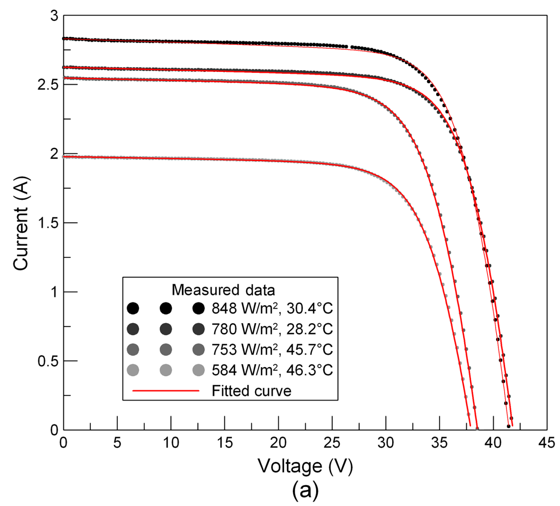

Figure 10. Measured data in different irradiation and temperature conditions and calculated curves according the proposed method for a monocrystalline silicon module.

- The iterative method for R_S determination always converges because the algorithm itself find a suitable value of m_R for the I–V curve (e.g. a-Si requires m_R larger than 2).
- The PV extracted parameters provide a highly accurate fitting for the I–V curves measured in all the temperature and irradiance conditions. In the maximum power region, the RMSD is less than 1% I_{SC} on average.

The method has also some important limitations such as the following:

- Being a method to extract parameters for an analytical equation considering a whole module, one should not

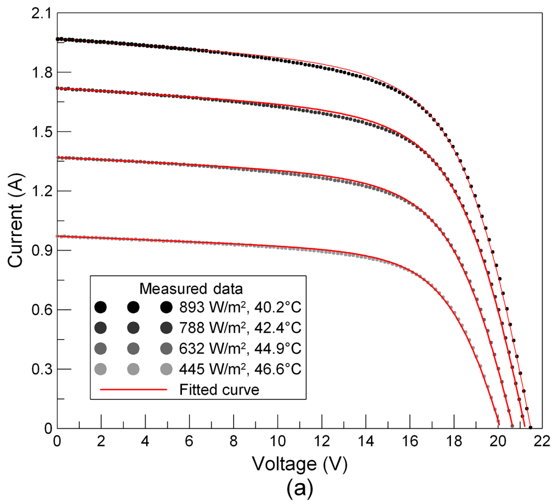

Figure 11. Measured data in different irradiation and temperature conditions and calculated curves according the proposed method for an amorphous silicon triple junction module.

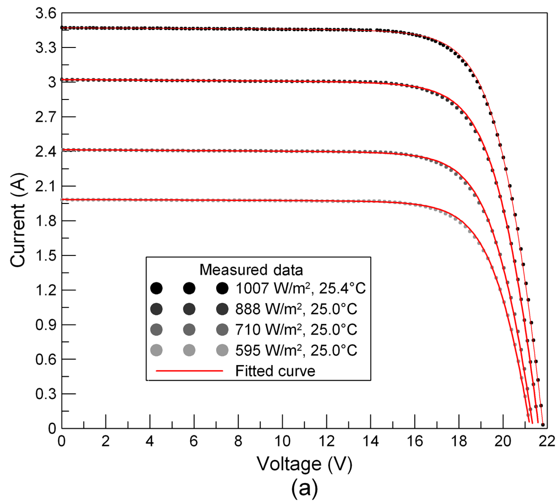

Figure 12. Measured data in different irradiation and temperature conditions and calculated curves according the proposed method for a multicrystalline silicon module.

Table I. Photovoltaic parameters extracted from *I–V* curves measured in different irradiation and temperature conditions for a Copper–Indium–Diselenide module with 42 cells connected in series.

Module: Shell Solar Eclipse 80 C, Cell technology: Copper–Indium–Diselenide							
Measurement conditions	I_{PH} (A)	R_S (Ω)	R_{SH} (Ω)	I_D (A)	I_R (A)	m_R	*RMSD* (% I_{SC})
766 W/m², 13.9 °C	2.104	2.765	327	1.018×10^{-20}	6.786×10^{-8}	2.62	0.39
570 W/m², 14.6 °C	1.558	2.764	514	2.927×10^{-20}	3.179×10^{-7}	2.87	0.39
412 W/m², 13.7 °C	1.156	3.211	475	3.392×10^{-20}	1.421×10^{-7}	2.75	0.44
279 W/m², 13.7 °C	0.739	4.274	1172	9.181×10^{-20}	1.315×10^{-6}	3.22	1.08

Table II. Photovoltaic parameters extracted from *I–V* curves measured in different irradiation and temperature conditions for an amorphous silicon single junction module with 108 cells connected in series.

Module: Kaneka G-EA060, Cell technology: amorphous silicon single junction							
Measurement conditions	I_{PH} (A)	R_S (Ω)	R_{SH} (Ω)	I_D (A)	I_R (A)	m_R	*RMSD* (% I_{SC})
656 W/m², 29.9 °C	0.704	15.014	1359	9.053×10^{-15}	1.219×10^{-4}	3.97	0.31
583 W/m², 34.1 °C	0.648	14.094	1822	1.846×10^{-14}	1.002×10^{-4}	3.71	0.78
430 W/m², 23.5 °*C*	0.511	16.807	2141	2.504×10^{-15}	1.153×10^{-4}	4.15	0.45
375 W/m², 26.3 °*C*	0.443	25.511	2033	5.117×10^{-15}	3.603×10^{-5}	3.59	0.40

Table III. Photovoltaic parameters extracted from *I–V* curves measured in different irradiation and temperature conditions for an amorphous silicon double junction module with 16 cells connected in series.

Module: Solarex Millennia MST-43LV, Cell technology: amorphous silicon double junction							
Measurement conditions	I_{PH} (A)	R_S (Ω)	R_{SH} (Ω)	I_D (A)	I_R (A)	m_R	*RMSD* (% I_{SC})
717 W/m², 25.1 °*C*	2.345	0.918	106	3.161×10^{-12}	6.658×10^{-4}	3.55	0.37
690 W/m², 35.5 °*C*	2.256	0.857	90	2.372×10^{-11}	5.866×10^{-4}	3.28	0.62
532 W/m², 25.2 °*C*	1.717	1.087	134	4.178×10^{-12}	6.189×10^{-4}	3.65	0.69
356 W/m², 20.8 °*C*	1.085	1.322	177	2.230×10^{-12}	2.077×10^{-4}	3.38	0.91

Table IV. Photovoltaic parameters extracted from *I–V* curves measured in different irradiation and temperature conditions for a HIT module with 72 cells connected in series.

Module: Sanyo HIP-200NHE1, Cell technology: HIT							
Measurement conditions	I_{PH} (A)	R_S (Ω)	R_{SH} (Ω)	I_D (A)	I_R (A)	m_R	*RMSD* (% I_{SC})
923 W/m², 23.4 °*C*	5.081	0.890	797	4.250×10^{-12}	5.413×10^{-7}	2.00	0.75
693 W/m², 18.8 °*C*	3.892	0.938	1927	1.943×10^{-12}	3.441×10^{-7}	2.00	0.81
575 W/m², 35.9 °*C*	3.216	0.863	3398	2.748×10^{-11}	1.347×10^{-6}	2.00	0.71
380 W/m², 17.5 °*C*	2.146	1.100	2663	1.700×10^{-12}	1.397×10^{-7}	2.00	0.75

HIT, heterojunction with intrinsic thin layer.

Table V. Photovoltaic parameters extracted from *I–V* curves measured in different irradiation and temperature conditions for a CdS/CdTe module with 116 cells connected in series.

Module: First Solar FS-272, Cell technology: CdS/CdTe							
Measurement conditions	I_{PH} (A)	R_S (Ω)	R_{SH} (Ω)	I_D (A)	I_R (A)	m_R	*RMSD* (% I_{SC})
984 W/m², 15.4 °C	1.157	17.120	1712	5.894×10^{-15}	9.682×10^{-6}	3.22	0.97
930 W/m², 14.7 °C	1.085	18.036	2052	6.065×10^{-15}	1.230×10^{-6}	3.31	1.11
745 W/m², 14.7 °C	0.880	19.902	1632	4.738×10^{-15}	1.715×10^{-7}	2.25	1.19
448 W/m², 14.3 °C	0.529	27.008	2407	4.631×10^{-15}	4.546×10^{-5}	4.05	1.16

Table VI. Photovoltaic parameters extracted from *I–V* curves measured in different irradiation and temperature conditions for a monocrystalline silicon module with 72 cells connected in series.

Module: Isofotón I-100/24, Cell technology: monocrystalline silicon							
Measurement conditions	I_{PH} (A)	R_S (Ω)	R_{SH} (Ω)	I_D (A)	I_R (A)	m_R	*RMSD* (% I_{SC})
848 W/m², 30.4 °*C*	2.837	0.857	394	6.970×10^{-10}	3.754×10^{-6}	2.00	0.52
780 W/m², 28.2 °*C*	2.628	0.840	519	4.377×10^{-10}	4.402×10^{-6}	2.00	0.41
753 W/m², 45.7 °C	2.550	0.890	579	7.455×10^{-9}	2.242×10^{-5}	2.00	0.43
584 W/m², 46.3 °C	1.980	0.967	735	8.211×10^{-9}	1.954×10^{-5}	2.00	0.41

Table VII. Photovoltaic parameters extracted from *I–V* curves measured in different irradiation and temperature conditions for an amorphous silicon triple junction module with 11 cells connected in series.

Module: Unisolar US32, Cell technology: amorphous silicon triple junction							
Measurement conditions	I_{PH} (A)	R_S (Ω)	R_{SH} (Ω)	I_D (A)	I_R (A)	m_R	*RMSD* (% I_{SC})
893 W/m², 40.2 °C	1.986	1.052	121	3.864×10^{-11}	8.913×10^{-5}	2.69	0.52
788 W/m², 42.4 °C	1.733	1.109	139	5.204×10^{-11}	6.548×10^{-5}	2.58	0.58
632 W/m², 44.9 °C	1.379	1.212	173	9.340×10^{-11}	5.748×10^{-5}	2.53	0.64
445 W/m², 46.6 °C	0.978	1.381	216	1.360×10^{-10}	2.048×10^{-5}	2.27	0.55

Table VIII. Photovoltaic parameters extracted from *I–V* curves measured in different irradiation and temperature conditions for a multicrystalline silicon module with 36 cells connected in series.

Module: Kyocera KC50T, Cell technology: multicrystalline silicon							
Measurement conditions	I_{PH} (A)	R_S (Ω)	R_{SH} (Ω)	I_D (A)	I_R (A)	m_R	*RMSD* (% I_{SC})
1007 W/m², 25.4 °C	3.472	0.294	955	1.867×10^{-10}	2.495×10^{-6}	2.00	0.36
888 W/m², 25.0 °C	3.023	0.324	783	1.950×10^{-10}	2.422×10^{-6}	2.00	0.40
710 W/m², 25.0 °C	2.415	0.362	833	2.102×10^{-10}	1.780×10^{-6}	2.00	0.46
595 W/m², 25.0 °C	1.983	0.377	1232	1.981×10^{-10}	1.638×10^{-6}	2.00	0.48

expect to find a suitable result in the case of a module with highly mismatched cells. It is possible to assume that all the cells are equal or that the analysis is applied on a virtual cell representing the average behaviour of all the cells in the module. In a case of a module with strongly mismatched cells, it is more suitable to apply a polynomial or a numerical expression. In the case of a module with small mismatches among the cells, the fitting quality is not significantly affected as shown in this work.

- Multijunction cells work in a similar way as cells connected in series, and as stated in item 1, mismatched cells may originate *I–V* curves in which the method is not suitable. In multijunction cells, because of changes in the spectral distribution, the behaviour of the association of the junctions can produce effects similar to the mismatched cells leading to a case in which the method is neither suitable.
- The diffusion diode ideality factor is assumed ideal ($m = 1$) that may be not appropriated in some cases like in a-Si devices because in this kind of materials, the conduction mechanisms may be more relevant as compared with conventional diffusion. However, the fitting quality of the proposed method is not affected by these mechanisms because the flexibility of the recombination diode values is high enough to compensate the possible inappropriate value of the diffusion diode factor.
- Although some of the PV parameters obtained from the proposed method, such as R_S and R_{SH}, are strongly associated to their physical values, the equations used in the method do not necessarily represent the actual behaviour of these parameters with irradiance and temperature. This happens because the method allows certain variability to their parameters to fit as best as possible each individually measured curve.

4. CONCLUSIONS

A method for PV parameter extraction according to a modified double-diode model was proposed. In this model, the ideality diode factor related to the recombination of the charge carriers is assumed as a variable with value equal or larger than 2. This method was applied to PV modules of different technologies in several of irradiance and temperature conditions. In all the studied cases, the PV extracted parameters provided a very good fitting with acceptable physical meaning. The RMSD for the fitting of the *I–V* curves was calculated, and it was less than 1% I_{SC} for almost all the modules. Only the CdTe module had a RMSD slightly larger than 1% I_{SC} although even in this case, the fitting can be considered good. It was also observed that for crystalline silicon modules, the parameter m_R can be assumed equal to 2; however, for thin film devices, the values must be larger.

ACKNOWLEDGEMENTS

The authors wish to acknowledge the National Council for Scientific and Technological Development of Brazil (CNPq) and the Brazilian Federal Agency for the Support and Evaluation of Graduate Education (CAPES) for the financial support and also the use of the facilities and the help of the staff of CIEMAT, especially Mr. Faustino Chenlo Romero.

REFERENCES

1. Chan DSH, Phang JCH. Analytical methods for the extraction of solar-cell single and double diode model parameters from *I–V* characteristics. *IEEE Transactions on Electron Devices* 1987; **34**(2): 286–293.
2. Garrido-Alzar CL. Algorithm for extraction of solar cell parameters from *I–V* curve using double exponential model. *Renewable Energy* 1997; **10**(2/3): 125–128.
3. Sandrolini L, Artioli M, Reggiani U. Numerical method for the extraction of photovoltaic module double-diode model parameters through cluster analysis. *Applied Energy* 2010; **87**: 442–451.
4. Nishioka K, Sakitani N, Uraoka Y, Fuyuki T. Analysis of multicrystalline silicon solar cells by modified 3-diode equivalent circuit model taking leakage current through periphery into consideration. *Solar Energy Materials and Solar Cells* 2007; **91**: 1222–1227.
5. Phang JCH, Chan DSH, Phillips JR. Accurate analytical method for the extraction of solar cell model parameters. *Eletronic Letters* 1984; **20**(10): 406–408.
6. Chan DSH, Phang JCH, Phillips JR, Loong MSA. Comparison of extracted solar cell parameters from single and double lumped circuit models. *Tech. Dig. 1st Int. Photovoltaic Science and Engineering Conf.*, Kobe, Japan, 1984; 151–153.
7. Charles JP, Mekkaoui-Alaoui I, Bordure G, Mialhe P. A critical study of the effectiveness of the single and double exponential models for the *I–V* characterisation of solar cells. *Solid State Electronics* 1985; **28**: 807–820.
8. Shockley W. 1949. The theory of P–N junctions in semiconductors and P–N junction transistors. *Bell System Technical Journal* **28**: 435–489 (reprinted in Sze S M 1991 Semiconductor Devices: Pioneering Papers World Scientific Publishing).